8.1 # WSR-88D OBSERVATIONS OF VOLCANIC ASH

Jefferson Wood* and Carven Scott
NOAA/National Weather Service, Anchorage, Alaska

David Schneider
U.S. Geological Survey-Alaska Volcano Observatory, Alaska Science Center, Anchorage, Alaska

1. INTRODUCTION

The eruption of Augustine Volcano during the period 11-28 January, 2006, presented a variety of challenges and opportunities for forecasters, scientists, and emergency managers throughout Southcentral Alaska. This event was the first time that a significant volcanic eruption was observed within the nominal range of a WSR-88D. The radar proved to be a crucial analysis and short term forecasting tool for meteorologists at the National Weather Service Forecast Office in Anchorage, Alaska and complemented the real-time geophysical monitoring conducted by the Alaska Volcano Observatory (Power et al., 2006). This paper will review some of the highlights of the volcanic events from the perspective of the radar data. In addition there will be a description of how the radar data were utilized in the operational forecast setting.

2. BACKGROUND

The hazards of volcanic ash are well documented. Volcanic ash is a significant hazard to aircraft operations (e.g. Hufford et al., 2000; Grindle and Burcham, 2003), as is the threat to public safety posed by volcanic ashfall (e.g. Horwell and Baxter, 2006; Stasiuk et al., 2003). Thus, timely detection and tracking of airborne ash is essential to a successful warning process during and immediately following an eruptive event. Real-time seismic monitoring can detect volcanic eruptions, but cannot determine how much ash is being produced, the height of the resulting ash cloud, or its movement. A variety of satellite techniques have been used successfully to track volcanic ash clouds; however, these techniques have certain limitations, as summarized by Marzano et al. (2006). The data are subject to limitations in both spatial and temporal resolution. Also, issues involving the detection of ash clouds using infrared brightness temperature differencing, a commonly used method, have been addressed by Simpson et al. (2000) and Prata et al. (2001), who suggest several scenarios where effective infrared satellite detection of volcanic ash clouds may be compromised. Prata et al. (2001) indicate that the brightness temperature differencing, also known as the 'split-window' method, can be subject to errors when the volcanic plume lies over a very cold surface, or when the plume lies above a clear land surface at night where strong surface temperature and moisture inversions exist. These scenarios can often be found over Alaska, particularly in the winter. In addition, the availability of visible satellite data is often severely restricted in the winter, due to the limited amount of daylight. This paper attempts to demonstrate the extensive potential of radar data in observing volcanic ash clouds.

Augustine Volcano is a 1,260 m high (4,134 ft) conical-shaped island stratovolcano located in southern Cook Inlet, about 290 km (180 mi) southwest of Anchorage, Alaska. Augustine is the most active volcano in the Cook Inlet region with five significant historical eruptions (1883, 1935, 1963-64, 1976, 1986) prior to 2006. These eruptions were primarily explosive events that produced volcanic ash clouds at their onset, followed by the emplacement of summit lava domes or flows. The explosive phase of the 2006 eruption consisted of thirteen discrete Vulcanian explosions from January 11 to 28, with seismic durations that ranged from one to eleven minutes (Power et al., 2006). These violent explosive events were characterized by the ballistic ejection of volcanic blocks and bombs, the emission of volcanic ash, and were accompanied by atmospheric pressure waves (Petersen et al., 2006). Cloud heights during this phase varied from 7.5 to 14 km above sea level. The character of the eruption changed to a more continuous ash emission phase from January 28 to February 2 that pro-

* *Corresponding author address:* Jefferson Wood, NOAA/National Weather Service, 6930 Sand Lake Rd., Anchorage, AK 99502; e-mail: jeff.wood@noaa.gov

-duced ash plumes at lower altitudes (below 4 km above sea level).

2. DATA

Unlike the majority of WSR-88D radars in the national radar network, Alaska radars are owned, operated, and maintained by the Federal Aviation Administration (FAA). NEXRAD Level III data from the Kenai, Alaska WSR 88-D radar were collected and used in this paper. The radar site is located on the western Kenai Peninsula, approximately 190 km northeast of Augustine volcano.

Level III data, as described in Crum et al. (1993), consist of the actual base products, e.g. base reflectivity, base velocity, and spectrum width, in addition to a selection of derived products including echo tops and Vertically Integrated Liquid (VIL). However, there are limits on the temporal availability of certain products. For example, composite reflectivity is available only every third volume scan at Level III while base reflectivity is available every volume scan. In contrast, Archive Level II data, which consists of the digital data output from the Radar Data Acquisition system, has the advantage of being a more complete data set that can be processed according to the specific needs of the user without the limited temporal resolution imposed by the Level III data. Level II data also allows for a wider array of products to be derived, whereas with Level III data, the user is limited to the archived product database. Unfortunately, Level II data is not available from Alaska WSR-88D platforms at this time. The base reflectivity data are of 1°x1km resolution, as are the base velocity and spectrum width data.

The archived data is provided by the National Climatic Data Center (NCDC) in Asheville, North Carolina. The radar images are created from this data set using the Java NEXRAD Viewer software, available from NCDC. The radar cross sections in the next section are recovered from the Anchorage Weather Forecast Office (WFO) local AWIPS database.

During the January 2006 Augustine eruption, the WSR-88D radar at Kenai operated in a variety of scanning modes, or Volume Coverage Patterns (VCPs). VCPs 12, 21, and 31, and 32 were the scanning modes employed during the course of the eruption. The specifications of each scanning mode are displayed in Table 1. Table 2 displays the altitude of the radar beam above Augustine volcano. The beam height is measured in kilometers above sea level, as opposed to above ground level.

VCP	Precip/ Clear Air Mode	Elevation Angles	Pulse Length	Time to Complete Scan
12	Precip	0.5, 0.9, 1.3, 1.8, 2.4, 3.1, 4.0, 5.1, 6.4, 8.0, 10.0, 12.5, 15.6, 19.5°	1.57 μs	4.1 min
21	Precip	0.5, 1.5, 2.4, 3.4, 4.3, 6.0, 9.0, 14.6, 19.5°	1.57 μs	6 min
31	Clear Air	0.5, 1.5, 2.5, 3.5, 4.5°	4.7 μs	10 min
32	Clear Air	0.5, 1.5, 2.5, 3.5, 4.5°	1.57 μs	10 min

Table 1 *– VCP specifications.*

Elevation Angle	VCP	Altitude above volcano (km)
0.5	12, 21, 31, 32	3.9 km
1.3	12	6.6 km
1.5	21, 31, 32	7.3 km
2.4	12, 21	10.2 km
2.5	31, 32	10.6 km

Table 2 – *Radar beam altitude above Augustine volcano for each elevation angle used.*

Table 3 (below) shows the scanning strategy that was employed for each of the 13 events during the eruption. One of the strengths of VCP 12 is the number of elevation scans at lower angles, providing for better vertical resolution of features in the lower levels. The higher density of lower elevation angles has the potential to be extremely useful in detecting ash from the Augustine volcano. However, the rapid scan feature of VCP 12 was available, allowing for total volume scans about every four minutes instead of the 6 minute interval with VCP 21 and 10 minute interval with

VCPs 31 and 32 (Table 1). Table 3 shows that VCP 31 was employed for the majority of the events following Event 3. The decision to employ VCP 31 was based upon the assumption that it would be better suited to detecting ash particles due to its greater sensitivity, a result of the longer pulse length and slower revolution of the radar antenna. This will be discussed in more detail later in the paper.

Event	Date	VCP	Elevation Angles Visible
1	1/11/2006	12	0.5, 1.3, 2.4
2	1/11/2006	12	0.5, 1.3, 2.4
3	1/13/2006	12	0.5, 1.3, 2.4
4	1/13/2006	31/12	0.5, 1.3, 1.5, 2.4, 2.5
5	1/13/2006	31	0.5, 1.5, 2.5
6	1/14/2006	31	0.5, 1.5, 2.5
7	1/14/2006	31	0.5, 1.5, 2.5
8	1/14/2006	31	0.5, 1.5, 2.5
9	1/17/2006	21/32	0.5, 1.5, 2.5
10	1/28/2006	31	0.5, 1.5, 2.5
11	1/28/2006	31	0.5
12	1/28/2006	31	0.5, 1.5
13	1/28/2006	31	0.5, 1.5

***Table 3** – VCPs employed during each eruptive event.*

3. RESULTS

a. Base reflectivity data

Each of the thirteen explosive events in January 2006 were observed by the WSR-88D at Kenai. A typical event (number 3) is visualized using the base reflectivity product in Figures 1 and 2. The radar was in VCP 12 for the entirety of this depicted event depicted in Figures 1 and 2. The first two frames of Figure 1 show the minutes preceding the explosion. Low reflectivity levels of around 5 to 15 dBz are shown over the volcano, indicating that low levels of ash are being emitted. According to Petersen et al. (2006), the Vulcanian explosion commenced at 1324 UTC. This is indicated in the last frame at 1328 UTC, when reflectivity levels above the volcano increase rapidly to 35 dBz.

The peak of the event on radar occurred 4 minutes later, at 1332 UTC (Figure 2). Reflectivity values of 55 dBz are observed in the 0.5° range and values of 35 dBz in the 2.4° slice, indicating that the ash plume ascended to at least 10 km asl. These high reflectivity values can be attributed to both the large volume of fine (<10 μm in diameter, as defined by Marzano et al., 2006) and coarse (between 10 and 64 μm) ash ejected as well as the high reflectivity of the larger lapilli (volcanic ash >1 mm in diameter) and volcanic bombs greater than 64 mm in diameter. The highest reflectivity values were limited to the lower portions of the plume (Figure 2). This may be due to the largest, most reflective ash particles falling out of the plume at this level, while smaller particles continue to ascend to the 2.4° elevation slice.

The 1332 UTC frame represents the peak of this event as seen on radar. By 1337 UTC, the reflectivity in the 2.4° slice diminished to around 5 dBz, although reflectivities in the 0.5° slice remained intense, with values of around 50 dBz observed. By 1345 UTC, radar returns were absent from 2.4°, while maximum values diminished further to 30 and 15 dBz at the 0.5 and 1.3° slices, respectively. This drop in reflectivity indicates that the larger and heavier, more reflective lapilli and volcanic bombs had fallen out of the ash plume (Marzano et al., 2006). It is also possible that ice accretion on the ash particles from the abundant water vapor ejected with the ash led to

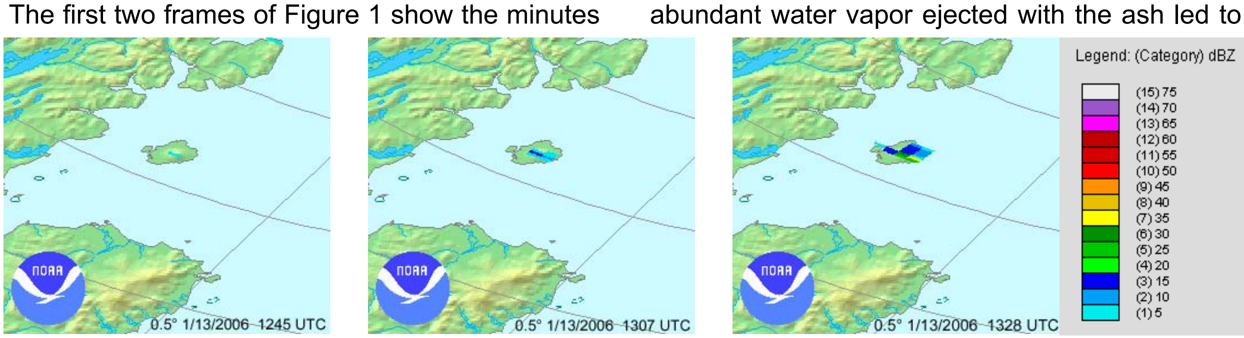

***Figure 1 –** 0.5° base reflectivity imagery from the Kenai WSR-88D at the onset of Event 3. Note the gradual increase in echoes between 1245 and 1307 UTC. The 35dBz maximum that occurs on the 1328 UTC image (far right) takes place 4 minutes after the start of the explosive event.*

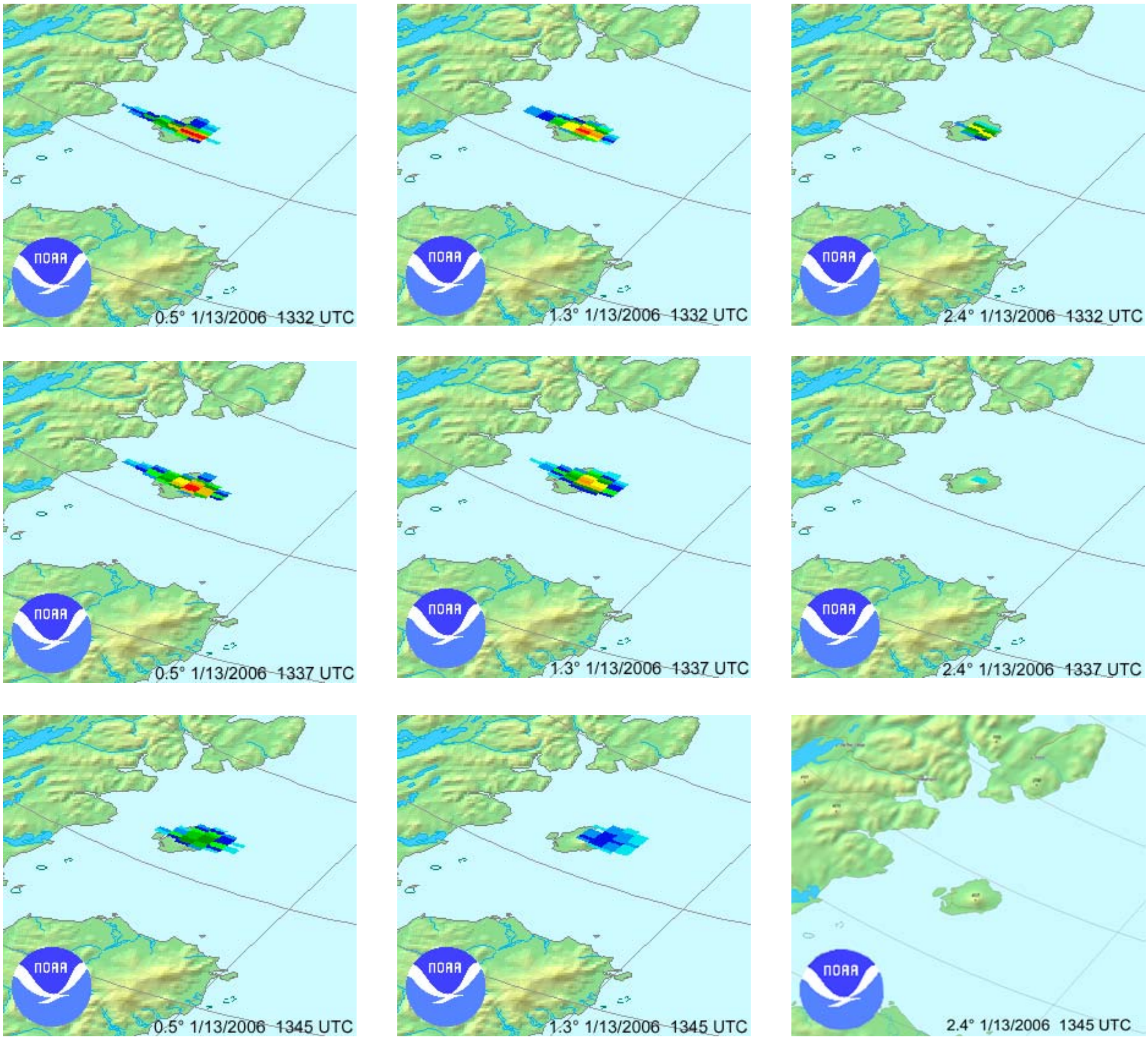

Figure 2 *– Base reflectivity for Event 3 at 0.5, 1.3, and 2.4° from 1332 UTC to 1345 UTC – the initial explosive phase of the eruption.*

the decrease in reflectivity observed because of the lower dielectric constant of ice, as discussed in Lacasse et al. (2004). The 1200 UTC January 13 sounding from Anchorage showed the altitude of the -15°C isotherm to be around 2.4 km. Given that the lowest altitude reflectivity observed above Augustine is 3.9 km at 0.5° elevation, it can be inferred that all of the observed ash was subject to ice accretion processes.

After 1345 UTC, the decline in reflectivity values and the height of the detected ash plume continued, as the ash cloud moved away from the volcanic source (Figure 3). Reflectivities continued to diminish in both strength and altitude, as indicated by the more rapidly decreasing echoes in the higher elevation angles. It may be that the stronger reflectivities in the lower elevation angles, particularly 0.5°, were due to the fallout from above. This is supported by the images at 1432 and 1454 UTC, shown in Figure 3. Reflectivity at 1432 UTC had weakened to the point that there is only one 10 dBz bin at 1.3° versus two 15 dBz bins at 0.5°. By 1454 UTC, reflectivity returns were absent from the 1.3° elevation scan and only one bin measuring 5 dBz remained at 0.5°. The diminishing of the reflectivity cores from the top down may suggest that the lower level returns were being sustained by fallout of heavier material from the upper levels of the ash plume. It is

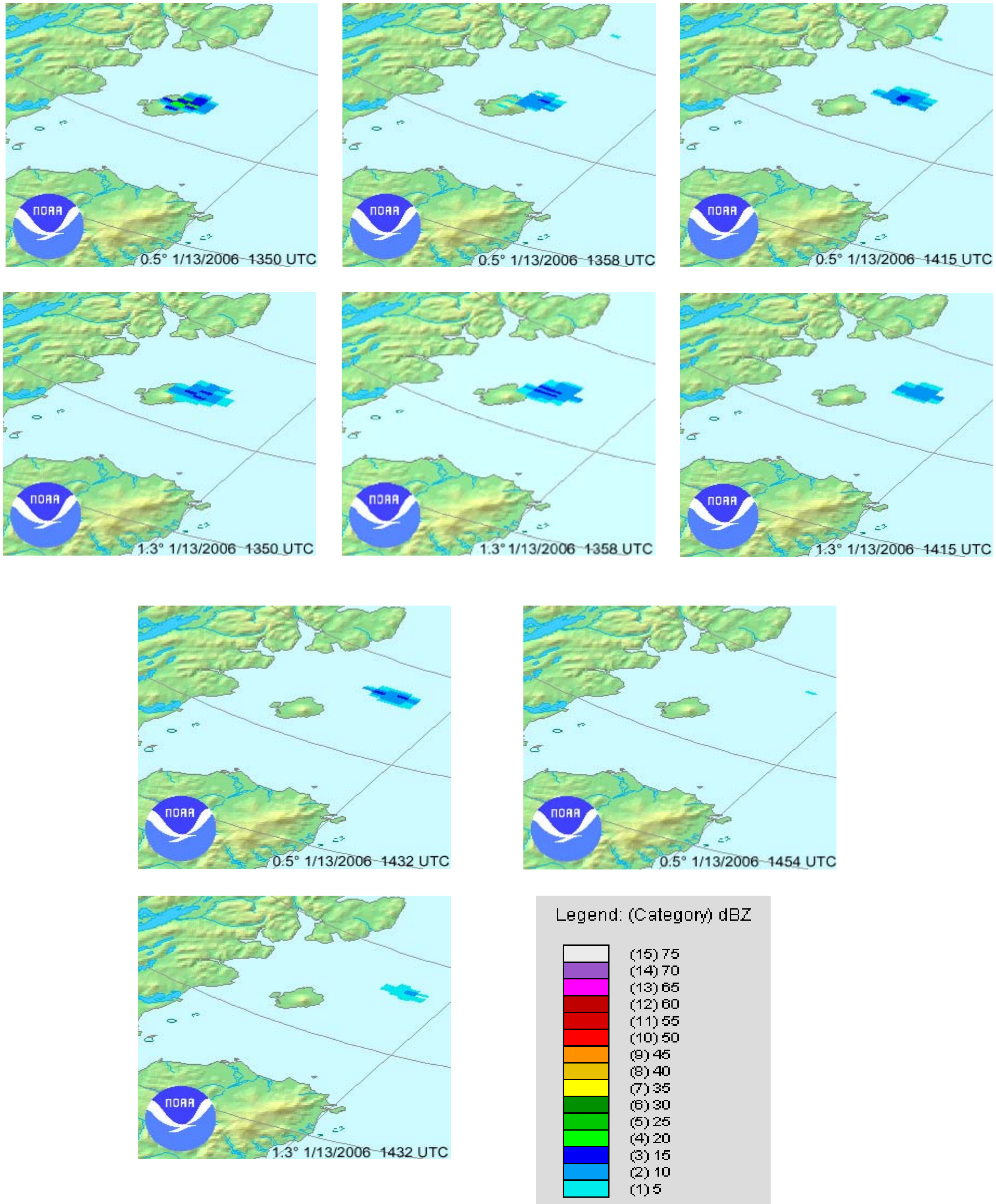

Figure 3 – *Base reflectivity at 0.5 (top row of each section) and 1.3° (bottom row of each section) elevation angles. The original ash plume is seen drifting northeast from the volcano as the event tapers off and the larger ash particles continue to fall out of the cloud.*

important to recognize, however, that the disappearance of the ash plume from the radar did not signify the end of the ash threat. Figure 4 displays IR satellite imagery from 1600 UTC that clearly shows the ash cloud from Augustine continuing northeast away from the volcano, over one hour after the cloud disappeared from the radar. By this point, the reduced concentration of ash, gravitational removal of larger ash particles, and ice nucleation and subsequent reduction of radar profile had rendered the cloud invisible to the WSR-88D.

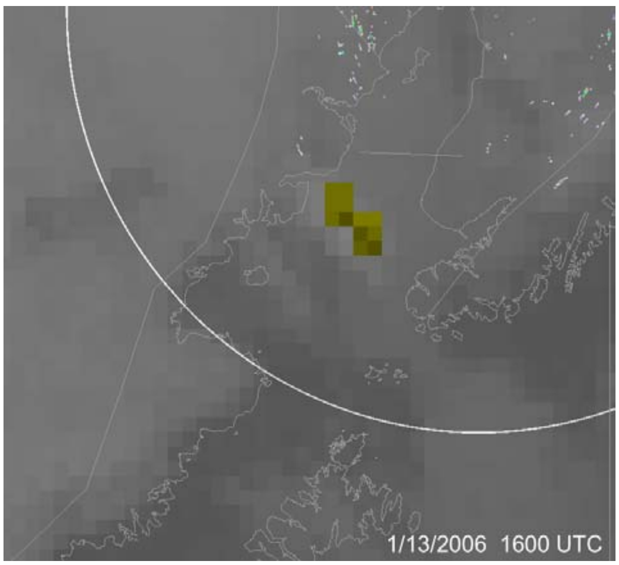

Figure 4 *– IR Satellite imagery 1600 UTC, over one hour after the last reflectivity image. The ash cloud from Augustine is still clearly visible.*

b. Base velocity and spectrum width data

In spite of the distance between the volcano and the radar (190 km), resulting in degraded resolution due to expanded beam width, the velocity data contains some interesting features. During several of the events, strong radial divergence can be noted in the base velocity product, an example of which is shown in Figure 5. This strong divergence signal can be seen again in Figure 6. This is consistent with what would be expected of an explosive event, which features radial divergence of material away from the volcanic vent. The turbulent flow associated with an explosive event appears in the spectrum width data, as seen in Figure 7. In this case, the high degree of variance within the range bins in the vicinity of the volcano implies turbulent flow.

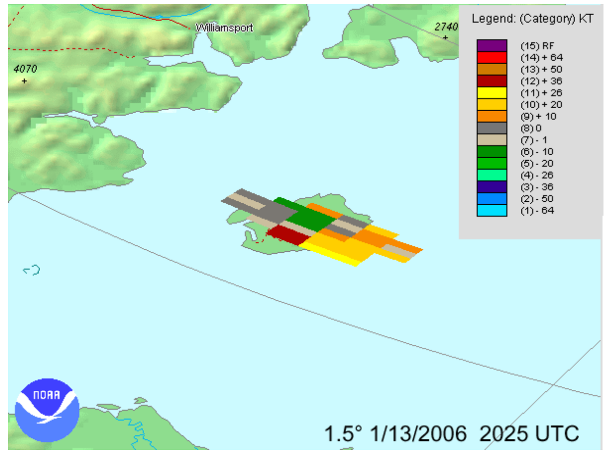

Figure 5 *– 1.5° base velocity product showing strong divergence approaching 50 kt (25.7 m/s) in the ash plume at approximately 7.3 km.*

c. VCP comparison

During the Augustine eruption, four VCPs were used by the WSR-88D; two in precipitation mode, and two in clear air mode. It can be seen from Table 2 that VCP 12 was the primary choice during the first four events (the radar was in VCP 31 at the beginning of Event 4, but immediately switched to VCP 12 at the onset of the eruptive event). After Event 4, the radar was placed in clear air mode, primarily VCP 31. This was done based on the assumption that the radar would better detect volcanic ash clouds as compared to VCP 12, as discussed in Section 2. Figure 8 below illustrates a method that was devised to compare the detection ability of the various VCPs by measuring the amount of time the ash clouds were detected by the radar for each event. The ash residence times were computed by measuring the time elapsed between the first appearance of reflectivity echoes over the volcano at the beginning of each event and the last frame in which echoes from the volcano are visible.

The VCP comparison results, as shown in Figure 8, indicate very little difference ash residency time between VCPs 31/32 and VCPs 12/21. Although the highest detection times were obtained in VCP 31 and 32, the mean residency times for VCPs 12/21 and 31/32 are 72.5 and 74.6 minutes, respectively. In comparing separate events of similar length that were viewed using VCP 12 and 31, it is noted that the events showed nearly identical progressions as described in Part a of this section. Figure 9 exemplifies this similarity. The last two 0.5° reflectivity

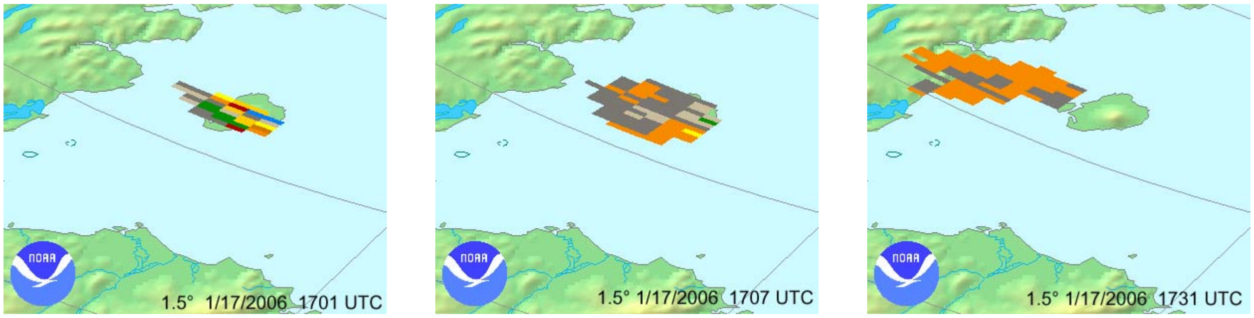

Figure 6 – *Another example of the base velocity product, this time from January 17. The strong divergence signal present in Figure 5 is once again present in the first frame. Six minutes later, the velocities have diminished considerably, although weak divergence is still visible on the southeast flank of the plume. By 1731 UTC, the divergence signal has disappeared, giving way to weak outbound velocities. The true velocities of the cloud at this point are most likely masked due to the perpendicular movement of the cloud relative to the radar beam.*

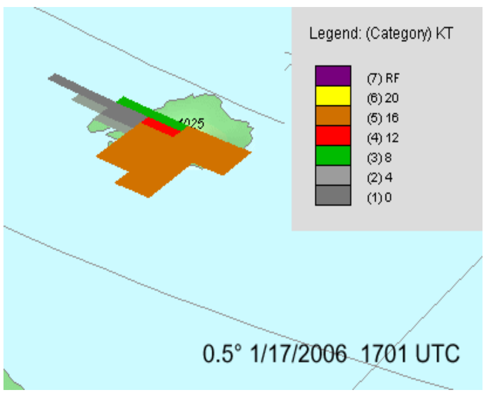

Figure 7 – *0.5° spectrum width product from January 17. Note the high spectrum width values at 0.5°, coincident with strong divergence from base velocity product in Figure 6.*

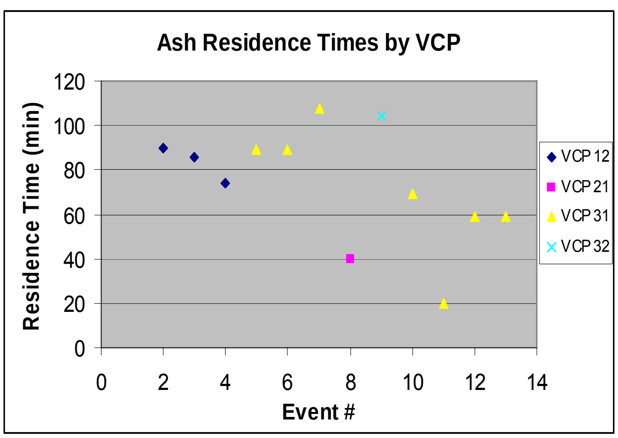

Figure 8 – *The number of minutes ash was detected by the radar during each eruptive event, categorized by VCP. Note that Event 1 is considered to have merged with Event 2, and thus is left out. Event 2 is considered to have started at the first detection of greater than 25 dBz reflectivity.*

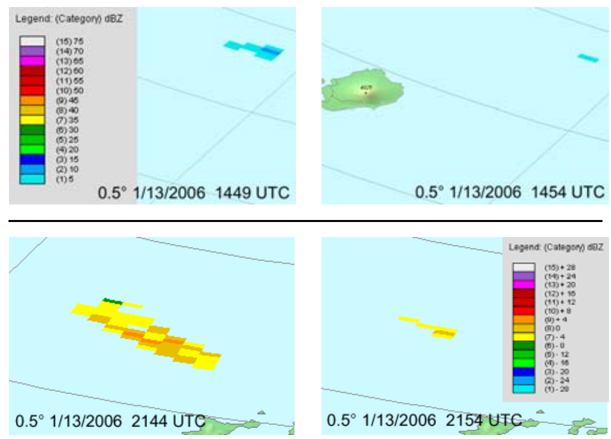

Figure 9 – *0.5° base reflectivity images from Event 3 (top) and Event 5 (bottom). The top two images are taken at 81(upper left) and 86 minutes (upper right) into Event 3. The bottom two images are taken at 79 (lower left) and 89 minutes (lower right) into Event 5.*

images from Events 3 and 5 are compared. Event 3 was observed in VCP 12 while Event 5 was observed in VCP 31. Both events had similar ash residency times at 0.5°: 86 minutes for Event 3 and 89 minutes for Event 5. It can be seen from Figure 10 that VCP 31 is better able to detect weaker echoes in the 0 to -4 dBz range than does VCP 12; as would be expected. The VCP 31 example also shows weaker echoes over a larger area than does VCP 12. However, as Figure 8 shows, there is little correlation between the VCP used and the length of time an ash plume is detected by radar.

One of the disadvantages to using VCP 31/32 in monitoring the eruption of Augustine was the rapid saturation that occurred in the early phases of each eruptive event. Figure 10 is a comparison of the initial stage of an eruption as viewed by

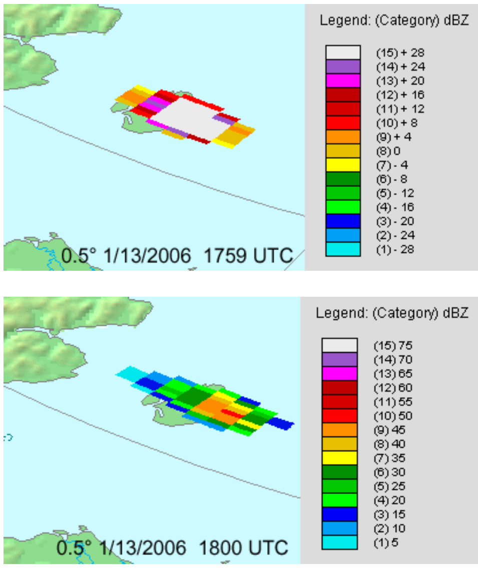

Figure 10 *– Comparison of VCP 31 (top) and VCP 21 (bottom) during Event 4.*

VCP 12 to one viewed by VCP 31. The presence of echo returns >50 dBz is not picked up by VCP 31, which is limited to returns under 30 dBz. This factor strengthens the case for keeping the radar in VCP 12 for volcanic events.

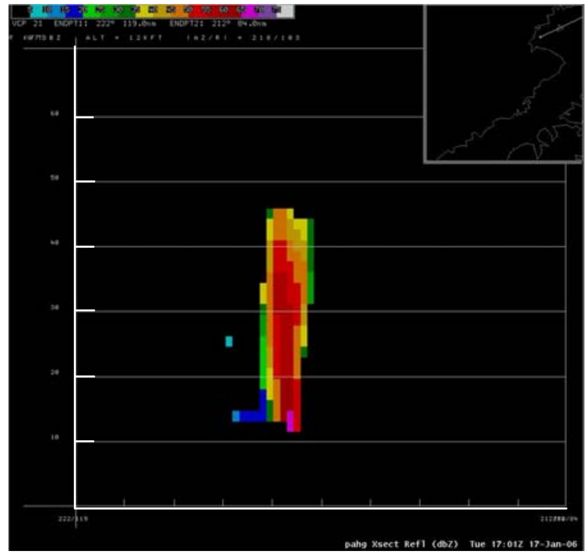

Figure 11 *– A reflectivity cross section from 1701 UTC, January 17, 2006. Each tick on the y-axis represents 10,000 feet asl (3.05 km). The ash plume reached a maximum height of over 14 km at the time this image was captured. Note that the reflectivity maximum is located at the bottom of the cross section. This is most likely due to the ejection of larger, more reflective material from the volcano.*

4. OPERATIONAL IMPACTS OF DATA

The utility of NEXRAD data was proven repeatedly during the Augustine eruption. The ability of the radar to provide near real-time updates on the position and altitude of volcanic ash clouds was vital in providing timely and accurate forecasts and warnings. One of the most significant contributions made by the radar data was in short term aviation forecasting. Radar cross sections were routinely used for diagnosing the vertical disposition of ash clouds during each event (Figure 11). These observations, in tandem with pilot reports, were used to ascertain the vertical extent of the ash clouds and issue timely advisories to the aviation community.

The ability to track the volcanic ash in the short-term was also vital to issuing timely and location-specific volcanic ashfall advisories. The ability to monitor the movement of the volcanic ash cloud on a minute by minute basis was essential given the close proximity of Augustine to settlements around the Cook Inlet region. In addition, marine weather statements were issued, alerting mariners to the potential hazards posed by the volcanic ash.

5. CONCLUSION

The eruption of Augustine Volcano in January 2006 provided a unique opportunity to showcase the capabilities of the WSR-88D in a context other than that for which the radar was originally designed. The radar data, in conjunction with pilot reports, proved to be crucial in analyzing the height and movement of volcanic ash clouds during and immediately following each eruptive event. The data greatly aided the National Weather Service and the Alaska Volcano Observatory in the issuance of timely and accurate warning and advisory products to aviation, public, and marine interests.

Reflectivity data from the WSR-88D showed that each explosive event was typically preceded by low level emissions of ash. The actual event usually commenced with a significant explosion, manifested in the radar imagery as a reflectivity spike, with the ash plume reaching its maximum height immediately or within minutes of the initial explosion. This phase was usually accompanied by a strong divergence signature in the base velocity data, with high variance in velocities appearing in the spectrum width data, suggesting a significant amount of turbulence, as would be expected with a volcanic explosion.

After the initial explosive phase of an event, reflectivity values tended to drop off. This was likely due to several factors, including a decrease in the amount of material being ejected by the volcano and the falling out of heavier, more reflective ash particles. Another compelling reason for the decrease in reflectivity is the accretion of ice on the volcanic ash, as suggested by Lacasse et al. (2004). Given the cold temperatures aloft at the time of the Augustine eruption, ice accretion is a viable explanation for the decrease in reflectivity seen after the initial phases of each event. The latter phase of each event was marked by a gradual tapering off of reflectivity values, generally within 90 minutes of the start of the event. However, IR imagery continued to detect the movement of the volcanic ash cloud well after its disappearance from the radar imagery. This highlights the continued importance of satellite imagery in tracking volcanic ash, particularly after the early stages of an eruptive event.

A comparison of the precipitation and clear air scanning modes shows little difference between VCPs 12/21 and 31/32 in the residency time of ash in the radar imagery. Although VCPs 31/32 do detect slightly weaker returns from the ash, the slight improvement gained in sensitivity is mitigated by the inability to detect reflectivities over 30 dBz. The greater density of lower level elevation angles that VCP 12 offers also makes it a more viable option, particularly in the earlier stages of an eruptive event. Ideally, a customized scanning strategy for volcano operations could be developed. Efforts have been undertaken in the past to develop new scanning strategies for the WSR-88D. Steadham et al. (2002) and Scott et al. (2003) propose a variety of scanning strategies that could be used for scanning volcanic events. Increasing temporal resolution of the radar data would also be of great use as well. A ‘flexible VCP’ that uses an algorithm to terminate a scan once two consecutive elevation angles have returns below a specified value, as described in Brown et al. (2000), could also be very useful in decreasing scan time and improving temporal resolution.

6. SUMMARY

Conclusions that may impact operations are summarized below:

- Current VCPs may not be optimal for the scharacterization of volcanic events. Therefore, the development of a new VCP that combines the enhanced low level elevation density and increased temporal resolution of VCP 12 with the enhanced sensitivity of VCP 31.

- Given currently available scan strategies, this preliminary investigation would suggest that it is advisable to use VCP 12 during the initial explosive phase of an eruptive event. Once the maximum reflectivity has dropped below 30 dBZ, VCP 31 should be used.

- This study clearly indicates that WSR-88D Level II data offers many advantages over Level III data currently available in Alaska. The ability to access this data would open up greater opportunities for research.

Given the proximity of WSR-88D platforms to active volcanoes in Alaska, as well as in the western Lower 48 states and Hawaii, radar data will likely play a major operational role when volcanic eruptions again pose a threat to life and property. The utilization of this tool to its maximum capability is vital.

7. REFERENCES

Crum, Timothy D., R. L. Alberty, and D. W. Burgess, 1993: Recording, archiving, and using WSR-88D data. *Bull Amer Met Soc*, **74**, 645-653.

Grindle, Thomas J. and F. W. Burcham, Jr., 2003: Engine damage to a NASA DC-8-72 airplane from a high-altitude encounter with a diffuse volcanic ash cloud. NASA Tech. Memo TM-2003-212030, 22 pp.

Horwell, Claire J. and P. J. Baxter, 2006: The respiratory health hazards of volcanic ash: A review for volcanic risk mitigation. *Bull Volcanol*, **69**, 1-24.

Hufford, Gary L., L. J. Salinas, J. J. Simpson, E. G. Barske, and D. C. Pieri, 2000: Operational implications of airborne volcanic ash. *Bull Amer Met Soc*, **81**, 745-755.

Klazura, Gerard E. and D. A. Imy, 1993: A description of the initial set of analysis products available from the NEXRAD WSR-88D system. *Bull Amer Met Soc*, **74**, 1293-1311.

Lacasse, C., S. Karlsdóttir, G. Larsen, H. Soosalu, W. I. Rose, and G. G. J. Ernst, 2004: Weather radar observations of the Hekla 2000 eruption cloud, Iceland. *Bull Volcanol*, **66**, 457-473.

Marzano, Frank S., G. Vulpiani, and W. I. Rose, 2006: Microphysical characterization of microwave radar reflectivity due to volcanic ash clouds. *IEEE Trans Geosci Rem Sens*, **44**, 313-327.

Petersen, T., S. De Angelis, G. Tytgat, and S. R. McNutt, 2006: Local infrasound observations of large ash explosions at Augustine Volcano, Alaska, during January 11-28, 2006. *Geophys Res Let*, **33**, L12303, doi:10.1029/2006GL026491.

Power, J.A, Nye, C.J., Coombs, M.L., Wessels, R.L., Cervelli, P.F., Dehn, J., Wallace, K.L, Freymueller, J.T., and Doukas, M.P.: The Reawakening of Alaska's Augustine Volcano. *EOS Trans Amer Geophy Union,* **87**, pp. 373, 377.

Prata, Fred, G. Bluth, B. Rose, D. Schneider, and A. Tupper, 2001: Comments on "Failures in detecting volcanic ash from a satellite-based technique. *Rem. Sens. Environ.*, **78**, 341-346.

Rose, William I., A. B. Kostinski, and L. Kelley, 1995: Real-time C-band radar observations of 1992 eruption clouds from Crater Peak, Mount Spurr Volcano, Alaska. *US Geol Surv Bull*, **2139**, 19-26.

Scott, Rhonda, R. M. Steadham, and R. A. Brown, 2003: New scanning strategies for the WSR-88D. *Preprints*, 19th International Conference on Interactive Information and Processing, Long Beach, CA, Amer.Met. Soc., P1.22.

Simpson, James J., G. Hufford, D. Pieri, and J. Berg, 2000: Failures in detecting volcanic ash from a satellite-based technique. *Rem. Sens. Environ.*, **72**, 191-217.

Stasiuk, Mark V., C. J. Hickson, and T. Mulder, 2003: The vulnerability of Canada to volcanic hazards. *Nat Hazards*, **28**, 563-589.

Steadham, Randy M., R. A. Brown, and V. T. Wood, 2002: Prospects for faster and denser WSR-88D scanning strategies. *Preprints*, 18th International Conference on Interactive Information and Processing, Orlando, Florida, Amer. Met. Soc., J3.16.